氏　　名	SOMSAK　TEERASAK
学位の種類	博士（工学）
学位記番号	博甲第９７０号
学位授与の日付	平成20年3月22日
学位授与の要件	課程博士(学位規則第４条第１項)
学位授与の題目	Conductive Microbead Detection Based on Eddy-Current Testing Technique with Giant Magnetoresistance Sensor（巨大磁気抵抗効果センサによるうず電流探傷技術に基づく導電性微粒子の検出に関する研究）
論文審査委員（主査）	山田　外史（環日本海域環境研究センター・教授）
論文審査委員（副査）	岩原　正吉（自然科学研究科・教授），上杉　喜彦（自然科学研究科・教授），木村　繁男（環日本海域環境研究センター・教授），飯山　宏一（自然科学研究科・准教授）

Abstract

This thesis describes the applications of spin-valve giant magnetoresistance (SV-GMR) sensor to detect the conductive microbead based on eddy-current testing (ECT) technique. The proposed ECT probes with SV-GMR sensor for detection of conductive microbead were fabricated. Three exciter coils were designed and developed for generating the magnetic field inside the conductive microbead; Helmholtz, Ferrite core and Flux concentrator. The signal variation of ECT signal is obtained from the detection of a microbead with range 125 to 380 μm radius at a frequency of 5 MHz. The signal obtained from SV-GMR sensor with flux concentrator is higher than signal obtained form double spiral, Helmholtz coil and ferrite core. Most of proposed probes can clearly detect the ball grid array (BGA) model. The result of finite element method (FEM) was calculated which agreed with the experimental result. In addition, one GMR clearly detects the magnetic particle model. Two GMRs were applied for one dimension underground water velocity detection. The simulation technique proved that in case of lift-off height the GMR can detect the signal at a good level. The results of simulations and experimentations have shown a great potential for this technique in future design and implementation. Furthermore, this technique is possible to detect the physical position.

1. Introduction

Eddy-current testing (ECT) technique is a well-known method of nondestructive evaluation technique that is usually applied to evaluate a material flaw without changing or altering the tested material. In addition, ECT technique is sensitive to material conductivity, which depends on many variables such as material thickness, crack, etc.. It is widely used in the aviation, nuclear power plant, automotive industries, electronic assembly, etc.

The GMR sensor has been applied to other applications except the data storage technologies because of its advantage as mentioned above. Detection of cracks or flaws on nonmagnetic material by GMR sensor based on ECT technique was proposed. Using GMR sensor instead of search coil is able to improve the probe sensitivity for crack or flaw detection and it also provides high-spatial resolution for applying it to microcrack detection. In addition, it is not difficult to develop a sensor array to improve the scanning time. Moreover, the ECT probe with GMR sensor can be applied to multi-frequency ECT system without changing the probe sensitivity.

In this thesis, three exciter coils were designed and developed for generating the magnetic field inside the conductive microbead; Helmholtz, Ferrite core and Flux concentrator. In addition, Two GMRs were applied for one dimension underground water velocity detection. The finite element method (FEM) and analytical method calculated the magnetic field distribution of ECT proposed probe and conductive microbead.

2. Spin-valve giant magnetorésistance characteristics

The SV-GMR characteristics were verified for capability of detecting magnetic field of the specimen. The direct current (DC) and small signal of SV-GMR characteristics are discussed as following.

Figure 1 shows the configuration of SV-GMR characteristics measurement. The apparatus of GMR test equipment consists of the Helmholtz coil, SV-GMR sensor, sources and data acquisition system. The normal resistance of SV-GMR is around 400 Ω.

2.1 DC characteristics

DC exciting current was fed to the Helmholtz coil within a range of -4 to 4 mT. The DC characteristics of the SV-GMR has maximum magnetic ratio approximately of 6 % of normal resistance or it has resistance variation between 1890 to 2010 Ω. The linear region sensitivity of the proposed SV-GMR is around 1.5 %/mT or 120 Ω/mT. And there is also a low hysteretic loop. Moreover, the proposed SV-

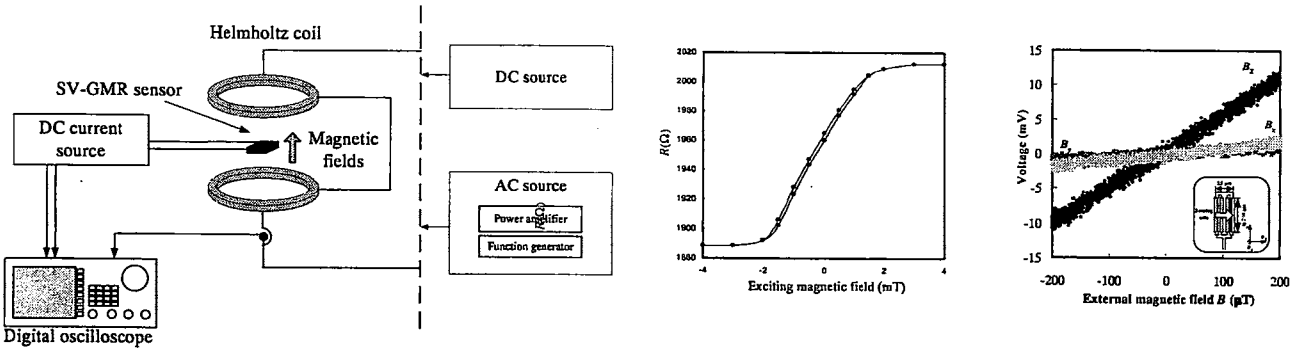

(a) Configuration of measurement (b) DC characteristics (c) small signal characteristics

Figure 1 Apparatus of GMR test equipment and its characteristics.

GMR sensor has high sensitivity with the applied magnetic fields ranging from -1 to 1 mT. The DC characteristic is shown in the Fig. 1(b).

2.2 Small signal characteristics

Figure 1(c) shows the small signal characteristics of the SV-GMR. The SV-GMR sensor was designed to have the most sensitive direction. However, some response was also expected for magnetic fields at the right angles to this direction. To determine the sensitive direction, the sensor was placed between the Helmholtz coils, but in three different orientations: with the sensitive direction aligned with the global *x*-, *y*- and *z*-directions. The magnetic field for these tests was driven at 100 kHz and with strength of ±200 μT. The SV-GMR sensor was biased with a constant current of 2.5 mA. A lock-in amplifier was used to measure the voltage difference across the terminals of the SV-GMR sensor. It is confirmed that the sensitive direction responded at 72μV/μT and this response was greater than the response of the other two directions (15 μV/μT).

3. Proposed probe with spin-valve giant magnetoresistance sensor [1]-[5]

3.1 ECT probe with Helmholtz coil exciter

3.1.1 ECT probe structure

The ECT probe configuration is shown in Figure 2(a). The probe consists of a pair of Helmholtz coil and a SV-GMR sensor. A copper wire of 0.2 mm diameter was used for making the

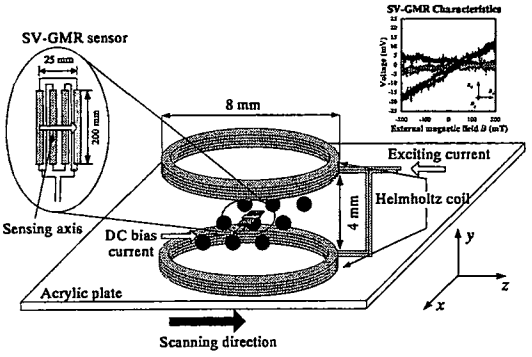

(a) ECT probe structure

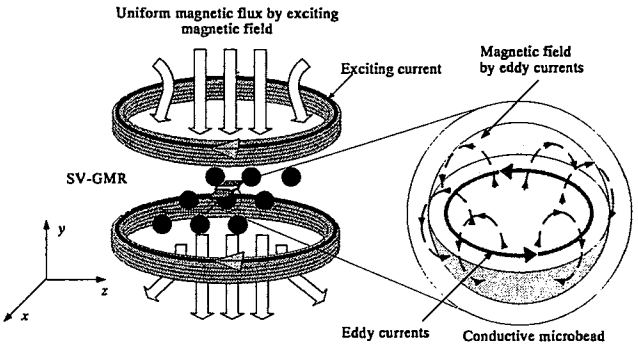

(b) Magnetic field distribution on ECT probe and conductive microbead

Figure 2 Structure and detection principle of proposed ECT probe.

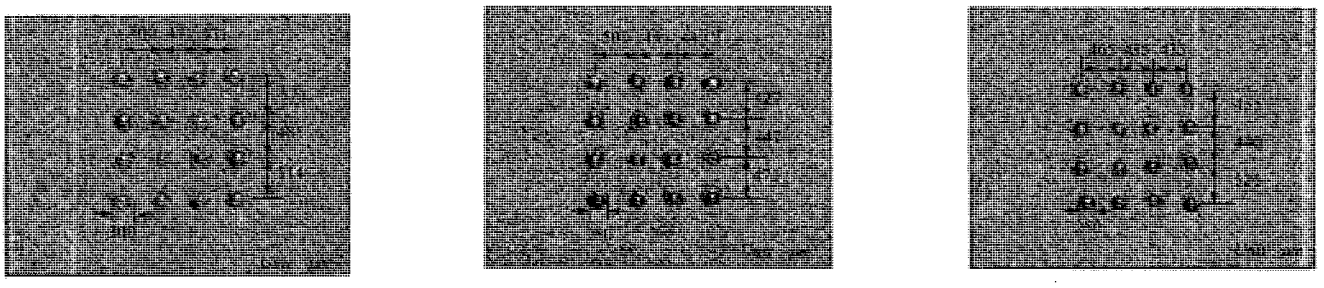

(a) Model I (b) Model II (c) Model III

Figure 3 Array of PbSn model.

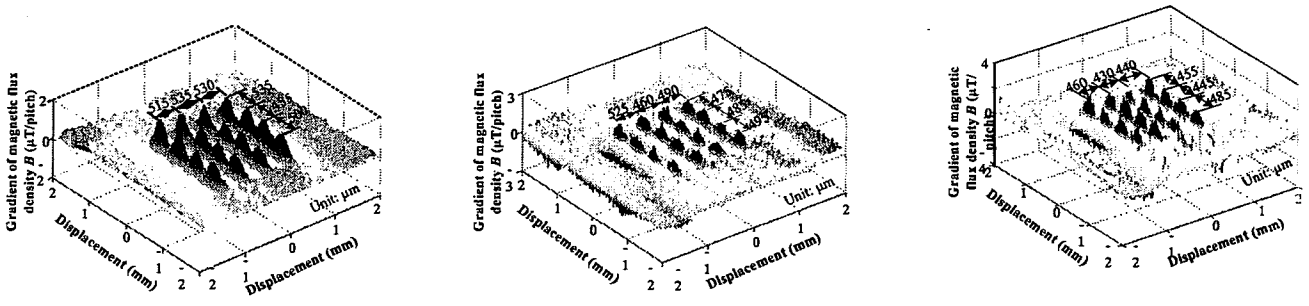

(a) Model I (b) Model II (c) Model III

Figure 4 3-D plot of measured signals.

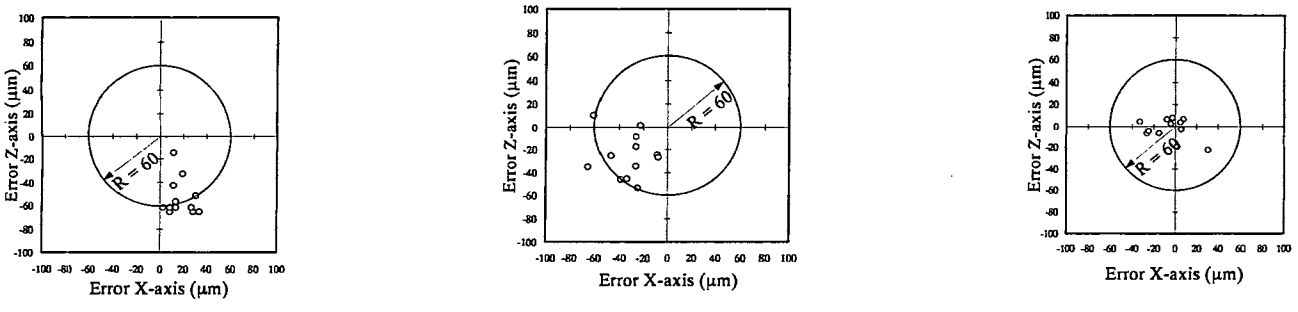

(a) Model I (b) Model II (c) Model III

Figure 5 Error plots of position calculation.

coils where the coil diameter was 8 mm and the number of turns was 4 turns. The upper coil and lower coil were connected in series. An AC exciting current of 200 mA was fed to generate the magnetic field. In this work, two exciting frequencies were used; 5 MHz and 10 MHz.

3.1.2 Detection principle

Figure 2(b) shows the principle of conductive microbead detection. An AC current was applied to the Helmholtz coil. The Helmholtz coil was chosen because it produces a reasonable homogenous and straight magnetic field which is normal to the planes of the coil. This magnetic field induces eddy currents in the conductive microbead. It is observed that the direction of eddy currents in the conductive microbead opposes the current flow in the exciting coil. The eddy currents in the conductive microbead generated a magnetic field. SV-GMR sensor detected the signal that was generated by eddy currents inside the conductive microbead. The microbead material was PbSn. For

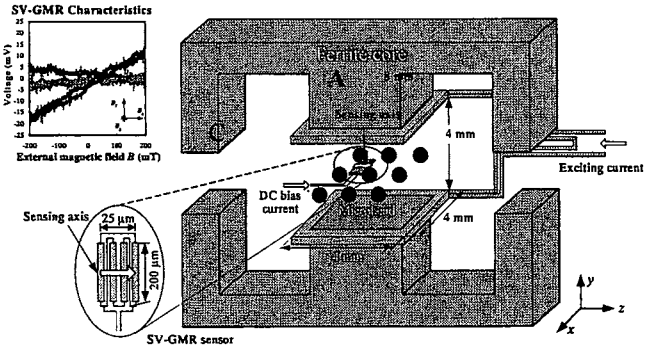

Figure 6 Proposed ECT probe structure.

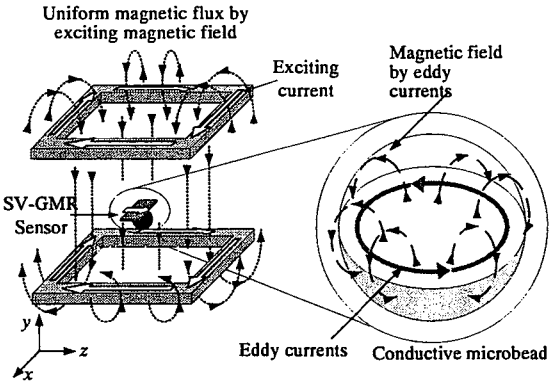

Figure 7 Principle of ECT probe.

the first experiments, a single microbead was used. In the single-microbead experiment, six beads were tested in the range from 125 to 380 μm (125, 150, 200, 250, 300, and 380 μm).

3.1.3 Investigation of the conductive microbead

Figure 3 shows the three array models, which are detected by Helmholtz coil excitation and SV-GMR sensor. From Figure 4 which shows the 3-D plot of measurement, we find that the positions of the microbeads in each array within the gradient magnetic flux density maps is distinct and could be used to estimate the microbead positions. Figure 5 shows the error of plot position estimation, the typical positional error of three arrays in the measurement is approximately 60 μm.

3.2 ECT probe with improved ferrite core exciter

3.2.1 ECT probe structure

The proposed ECT probe consists of the SV-GMR as a sensor and an exciter as shown in Figure 6. The copper wire of 0.2 mm diameter was used for making coils and the number of turns was four turns. The copper wire was wound on the ferrite core with squares of 4 mm length. The upper and lower was connected in series. The distance between upper and lower had four mm. The conductive microbead was laid on the mid of upper and lower coil. Sensing axis of the SV-GMR sensor is z-axis. The exciting current of 200 mA was fed to the exciter for generating the magnetic field. In this work exciting frequency of 5 MHz was used.

In all experiments, the microbead material was Pb-Sn solder. For the first experiments a single microbead was used. In the single-microbead experiments six radiuses were tested (125, 150, 200, 250, 300 and 360 μm). For the second model, the microbeads were arranged in a single row. Three

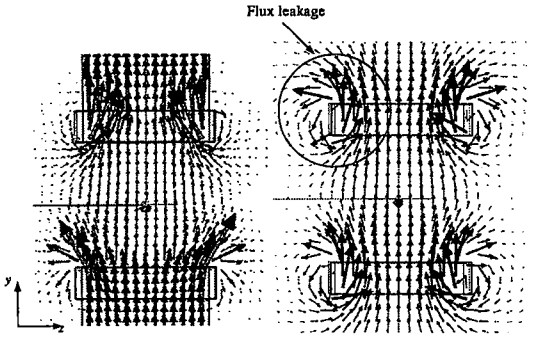

Figure 8 Flux leakage of proposed probe and reference probe.

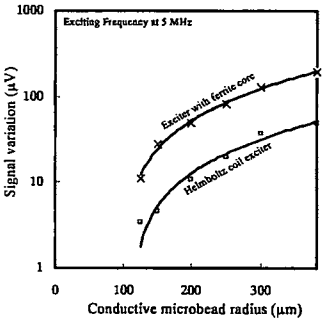

Figure 9 Signal variations of proposed probe and reference probe.

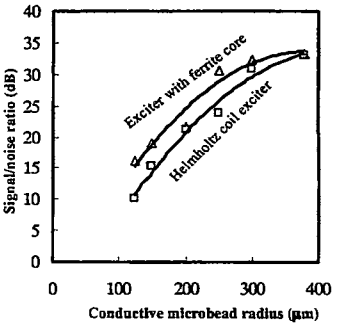

Figure 10 Signal to noise ratio of proposed and reference probe.

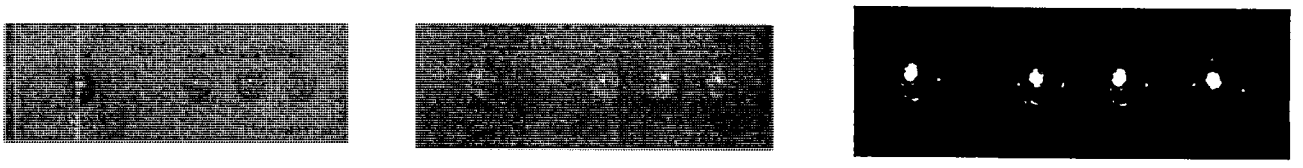

(a) Model I (b) Model II (c) Model III

Figure 11 Conductive microbead row model.

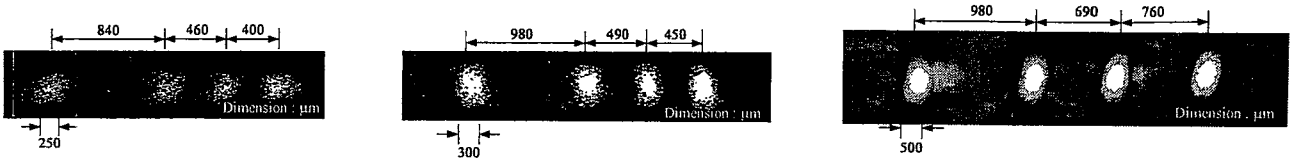

(a) Model I (b) Model II (c) Model III

Figure 12 2-D map of detection of microbead row model.

microbead radiuses were used (125, 150 and 250 μm) with different pitch in the range from 400 to 1000 μm.

3.2.2 Detection principle

Exciting current with frequency 5 MHz was fed to the exciter. The exciter construction was chosen because it produced a reasonably homogenous and straight magnetic field which is normal to the planes of the coils. Figure 7 shows arrangement of ECT probe and microbead. The exciter generates magnetic fields which induces eddy currents in the microbead. The eddy currents in the microbead generated a magnetic field as shown. The detection approach was to measure the z-axis component of the magnetic field generated by the microbead eddy-currents.

Figure 8 shows the flux leakage of proposed probe and reference probe calculated by finite element method (FEM). The reference probe was fabricated as the Helmholtz coil. The proposed probe can decrease the flux leakage because it used the core made with ferrite material. The magnetic flux generated by proposed probe can be higher than reference probe. The properties of ferrite material can increase the magnetic flux for the reason that it had permeability higher than air core. For this reason, the proposed ECT probe was fabricated that improved signal for SV-GMR.

3.2.3 Investigation of the conductive microbead

Single microbeads with six radiuses were detected (125, 150, 200, 250, 300 and 360 μm) by both of reference and proposed ECT probe. Both probes were fed the same power which means that the probe can generate equal magnitude of magnetic flux. The signal variation of both reference and proposed ECT probe are expressed in Figure 9. The effect of bead signal of proposed ECT probe is approximately four times higher than the reference probe because of the property of core material.

Thus, the proposed exciter coil can increase flux density directly to bead.

The signals of SV-GMR obtained form the ECT probe contains not only signal of microbead detection but also noise. Figure 10 presents the signal to noise ratio (S/N) of reference and proposed ECT probe. The calculation of S/N ratio of both reference and proposed probe expresses the proposed ECT probe has low noises signal. The model of microbead row was fabricated with three radiuses (125, 150 and 250 μm) with pitch range from 400 to 1000 μm as shown in Figure 11.

Figure 12 shows the 2-D plot of measurement; we find that the microbead position of each model within the gradient magnetic flux density maps is distinct and can be used to estimate the microbeads positions.

3.3 ECT probe with flux concentrator

3.3.1 ECT probe structure

Figure 13 shows the struture of the proposed ECT probe that consists of the SV-GMR sensor and flux concentrator. The inside and outside diameter of exciter coil or flux concentrator are 2 and 5 mm respectively. The conductive plate was laid between the upper-lower spiral coils. The conductive plate with 0.1 thinckness was chosen because of its effect from skin depth.

The upper-lower spiral coils were connetecd in series. An exciting current of 200 mA was fed to the coils to generate the magnetic fields. In this work the exciting frequency was 5 MHz. The *z*-direction of the coordinate system used in this work was define as the direction of scanning direction. The SV-GMR sensor was positioned so that the sensing axis was at right angles to the magnetic fields generated by the flux concentrator. The closest approach of the SV-GMR sensor to the specimen was thus limited to 100 μm.

3.3.2 Detection principle

Figure 14 shows the structure and magnetic field distribution on ECT probe and conductive microbead . An ECT probe was constructed using a flux concentrator for excitation. Exciting current was fed to flux concentrator coil to generate a magnetic field. The conducting plate, which is the key element of exciter, has an air hole in its center and slit in the radial direction. When the exciting current is applied, a magnetic field is produced in the air gap and eddy currents are induced in the conducting plate.

It is evident from Figure 15 that (when there is no slit in the conducting plate), the eddy currents flow mainly towards the outer portion of the plate and the net flux near the center of inner portion of the plate is almost nil. This is due to the fact that at the inner portion of the plate the induced mmf and the exciting mmf oppose one another or in other words, the exciting flux and the flux due to eddy currents oppose each other. The presence of slit forces the eddy currents to flow around the air hole. As a result the exciting flux and the flux due to eddy currents act in the same direction. It means that the total magnetic flux over the conductive microbead equal flux generated by exciting coil plus magnetic fields generated by eddy currents from conducting plate.

A specimen such as a conductive microbead was placed over the flux concentrator coil and sensor. The flux concentrator coil generated magnetic field and induced eddy currents to flow inside the microbead, where the signal generated by SV-GMR was detected.

3.3.3 Investigation of the conductive microbead

The system configuration described above was designed to produce a magnetic field near the conductive microbead and SV-GMR. FEM model was used to check that this was achieved. The model parameters included exciting current 200 mA at 5 MHz. The physical arrangement of the model elements simulated the real equipment as described above. The with and without conducting plates

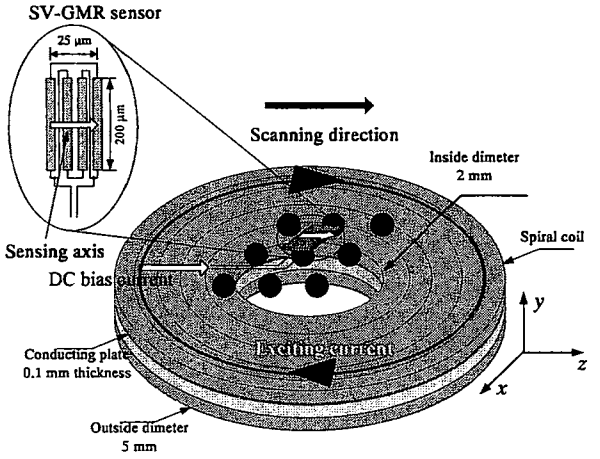

Figure 13. ECT probe structure.

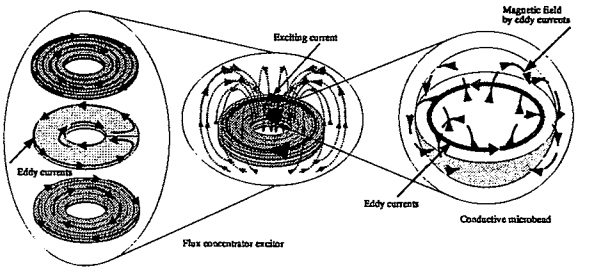

Figure 14. Magnetic field distribution on ECT probe and conductive microbead

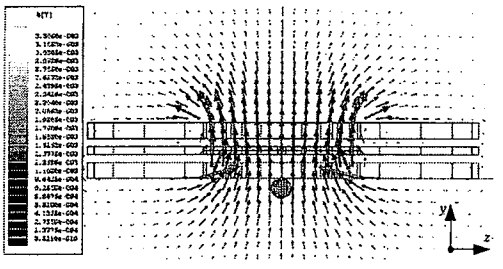

Figure 15. Magnetic filed distribution calculated by FEM.

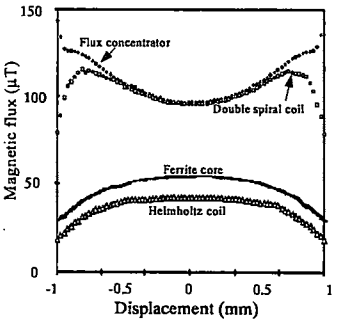

Figure 16. Magnetic flux at the center of four exciter coils.

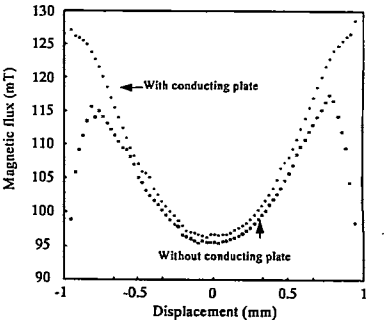

Figure 17. Magnetic flux at the center of with and without copper plate.

were chosen for evaluation to generate the magnetic flux at conductive microbead. Maxwell 3D software version 10 from Ansoft Corporation was used.

Figure 15 shows a plot of magnitude of the magnetic field vector on *y-z* plane of flux

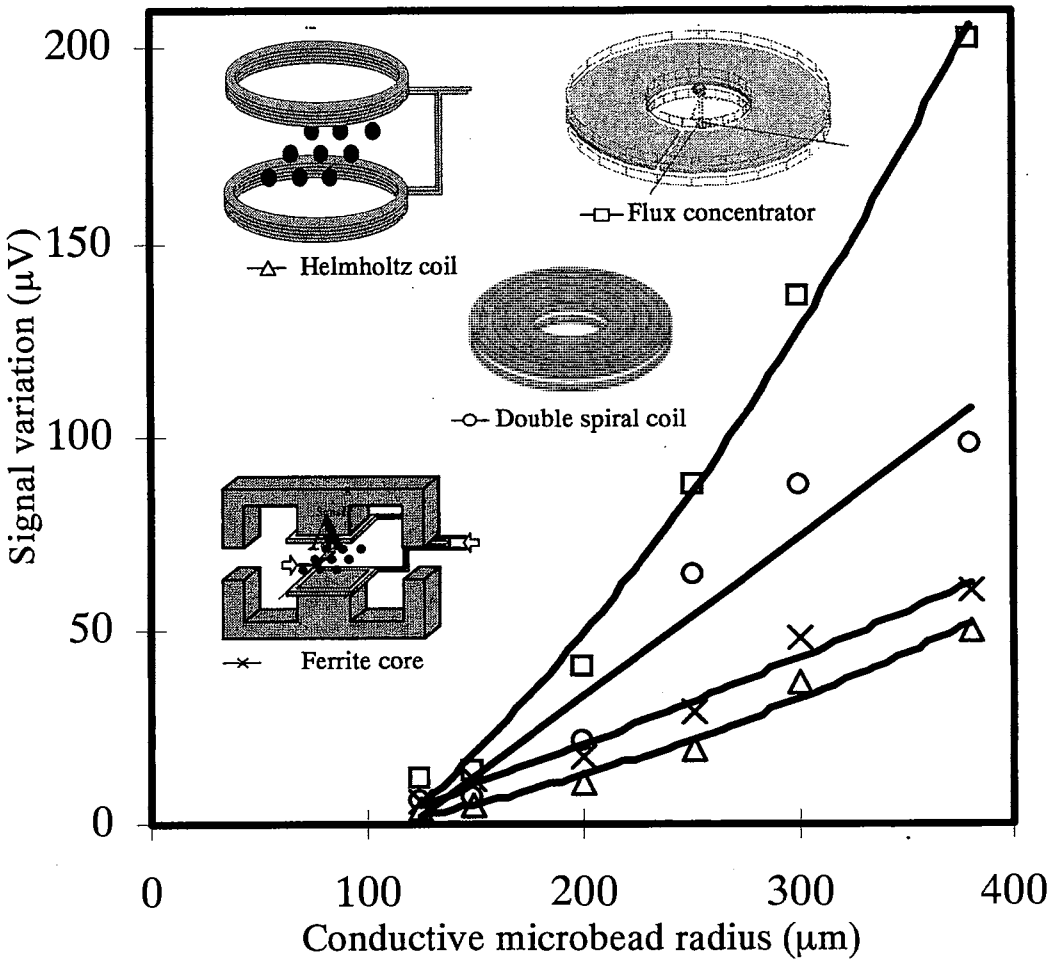

Figure 18 Signal variation of detection conductive microbead signal with various exciter coils.

concentrator with conductive microbead of 125 μm radius, as calculated by the Maxwell FEM software. According to the software the field is quite smooth near the centre of the coils.

The FEM calculated the magnetic flux at the center in the middle of exciter coil. The four models (flux concentrator, double spiral, Helmholtz coil and ferrite core) were calculated to express the magnetic flux. Figure 16 shows the result of magnetic flux at the middle of the three exciter coil models. The calculation shows the flux concentrator generated magnetic flux higher than double spiral and Helmholtz coil, around 1.22 % and 130 % respectively. Figure 17 expresses the result of magnetic flux in the middle with and without copper plate.

3.4 Comparison of Signal result of three proposed ECT probes.

The ECT probe scanned over the model with 20 μm scanning pitch and lock-in amplifier was used to measure the ECT signal obtained from SV-GMR sensor. The signal variation of ECT signal in Figure 18 is obtained from the detection of a microbead with range 125 to 380 μm radius at the frequency of 5 MHz. The flux concentrator, double spiral, Helmholtz coil and ferrite core were used as an exciter. The signal obtained from SV-GMR sensor with flux concentrator is higher than signal obtained form double spiral, Helmholtz coil and ferrite core. This agrees with the calculated results obtained from FEM calculation. The experimental results also show that signal variations at the microbead depend on the frequency of the exciting magnetic fields and the microbead radius.

The proposed ECT probe that was fabricated consists of the SV-GMR as a sensor and exciter. The flux concentrator, double spiral, Hemholtz coil and ferrite core were compared to detect the conductive microbead. The proposed ECT probe (flux concentrator) can improve the signal obtained from the SV-GMR sensor. The result of FEM was calculated which agreed with the experimental result.

4. Detection of micro material [6]-[7]

4.1 High frequency technique detection of micro conductive microbead

4.1.1 ECT probe structure and principle detection

Figure 19 shows the ECT probe structure and magnetic fields distribution. ECT probe was constructed using a planar meander coil as an exciter. The SV-GMR sensor was positioned so that the sensing axis was at right angles to the magnetic fields meander coil to generate a high frequency magnetic field.A specimen such as a conductive microbead was placed below the meander coil and sensor. The meander coil magnetic field caused eddy currents to flow in the microbead, which in turn generated a small magnetic field which was detected by the SV-GMR sensor. The planar coil had a line 200 μm width and had a gap between lines of 50 μm width. The meander coil was 35 μm thick and was protected by a 50 μm polymer film on both upper and lower sides. The closest approach of the SV-GMR sensor to the specimen was thus limited to 135 μm.

4.1.2 Recognition result

The ECT probe scanned over the model with 20 μm scanning pitch and lock-in amplifier was used to measure the ECT signal obtained from SV-GMR sensor.

Figure 20 shows the maximum variation of the ECT signal versus the radius of the microbead ranged from 125 to 300 μm. The maximum signal variation at exciting frequency of 10 MHz decreases with the microbead radius and it is lower than the signal variation at exciting frequency of 5 MHz when the microbead radius is larger than 200 μm. This is because the planer meander coil cannot generate the uniform magnetic field distribution.

4.2 Ferromagnetic material detection

4.2.1 Experimental setup

In case of ferromagnetic material detection, the high frequency method and static magnetic field were applied to recognize the magnetic particle. The ECT probe (refer to Figure 19) for detecting the non-magnetic material was used for detection of the ferromagnetic material. The exciting frequency with 5 MHz was fed to the planar meander coil as an exciter for generating magnetic field.

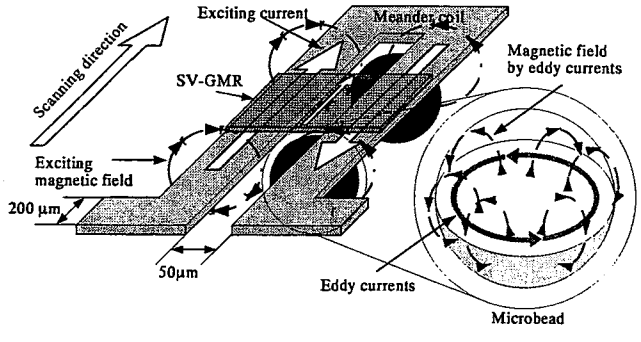

Figure 19 ECT probe structure.

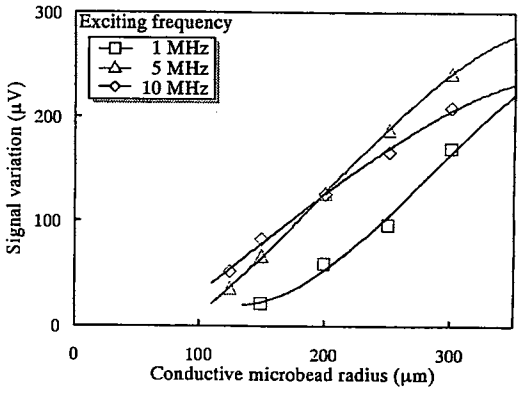

Figure 20 Signal variation vs. microbead size.

The ferromagnetic field was laid under the planar meander coil and SV-GMR sensor. We use the speed of ECT probe over the magnetic particle scanning with 0.5 mm/min.

Figure 21 shows the probe construction. The static magnetic fields around 100 mT were applied to magnetic material to magnetize the magnetic material. The SV-GMR sensor is also set so the sensing axis will detect only the *z*-axis component of magnetic fields. Wheatstone bridge is used to eliminate the offset voltage. The distance between the SV-GMR sensor and magnetic material was at least 50 μm. The SV-GMR sensor is scanned over the magnetic material with speed of 1 mm/min.

The magnetic particle model is made from Fe. The Fe is laid on an acrylic substrate and fixed with liquid glue. The magnetic particle size are 20, 40 and 60 μm.

4.2.2 Recognition results

Figure 22 shows the magnetic particle model and its results by using the ECT method. We found that the signal over the reference line can recognize the magnetic particle of only 40 and 60 μm

size, because of the high lift-off between SV-GMR to magnetic particle. The 2-D image plot shows the signal of the SV-GMR sensor where is possible to detect the magnetic particles.

Figure 23 shows the magnetic particles model and its recognition results. The signal over the reference line shows the variation of signal wherever the magnetic particle exists. The 2-D image obtained from scanning result also shows the utilization of the SV-GMR sensor to detect the magnetic particle clearly.

According to the results of ferromagnetic material detection, we found that both of the high

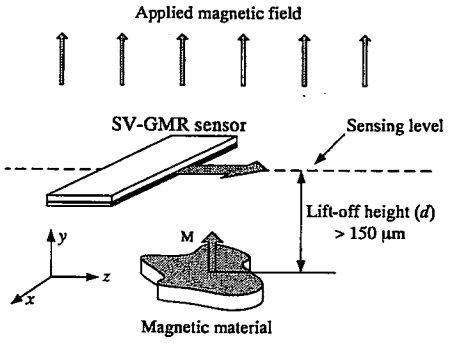

Figure 21 Recognition of Fe by SV-GMR with static magnetic field.

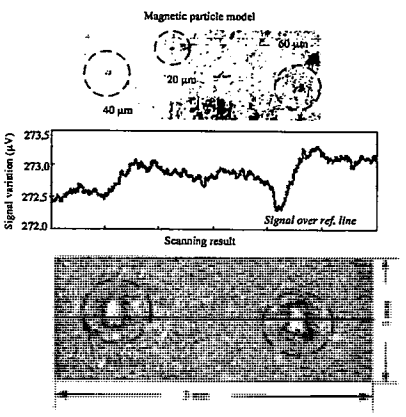

Figure 22 Magnetic particle model and its results by using the ECT method.

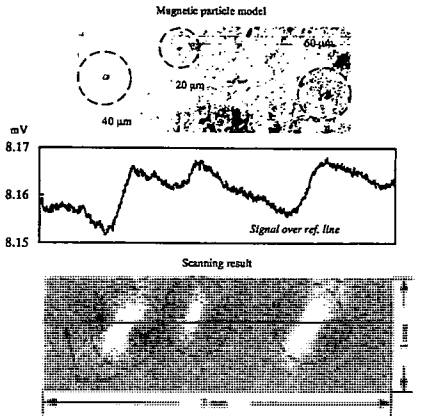

Figure 23 Magnetic particle model and its results by applied static magnetic field.

frequency method and static magnetic field method can recognize the specimen. In the case of high frequency method, this technique enables us to detect smaller ferromagnetic material if the GMR sensor is kept more close to specimen.

The analytical and experimental results show that the SV-GMR can be applied to detect the non-magnetic (conductive) material both of single and array with 125 μm radius based on ECT technique. In the case of ferromagnetic material detection (Fe, size of 20-60 μm), the high frequency method and static magnetic field were applied to recognize the magnetic particle. All of the experiment results confirm that the SV-GMR sensor can be applied to detect micro magnetic material and ferromagnetic material. The results indicate that the SV-GMR is useful and possible to use in physical measurement.

5. Underground water velocity detecting magnetic particle [8]

The effect of underground water contaminated from the industrial area and nuclear power plant waste is considered as an environmental issue. The behavior of underground water is essential to monitor the potential of qualitative and quality. In general, the velocity of underground water is very low around 10-6–10^{-8} m/s. There are many kinds of methods that can monitor the underground water behavior such as thermal conductivity, ultrasonic etc.

Spin-valve magnetoresistance (SV-GMR) sensor is selected to be used as a sensor because it has high sensitivity and high resolution, ranging from nanotesla to several millitesta, and provides good performance versus cost. In recent years, the SV - GMR sensor has been successfully applied to detect the flaw on printed circuit board and conductive microbead array. This section describes the underground water velocity measurement using SV-GMR sensor.

The proposed model of underground water measurement consists of the two GMRs as a sensor and a magnetic particle reservoir as shown in Figure 24. The fixed distance between GMR is 400 μm. The magnetic particle has a size of range 1 - 100 μm and has difference dipole moment direction. The concept is determining the one-dimension velocity by using the detected GMR signal from the magnetic particle over the GMR-I and II.

5.1 Detection of underground water velocity by GMR

Magnetic particles have a lot of environmental effect such as the pattern flow of underground

water, conductivity of water, contamination, specific gravity of water and etc.. In order to demonstrate the feasibility of the proposed technique, experiments and simulations are performed.

The experiment was set by using two GMRs to detect the magnetic particle model III to represent the particle flow in underground water. The experiment was set by fixing the magnetic particles and moving the GMR scanning in *x-y* plan and the signal obtained from GMR collected to PC. The distance between GMR I and II was fixed at 400 μm.

In this study, only one-dimension is considered. We assume the density of magnetic particle is as close as to the water source. In case of particles sink effect in real application, it is possible to find out the high range of weight distribution and particle density value close to water source.

5.2 GMR signal matching

The two GMRs were applied to detect the magnetic particle model III. The result of correlation statistics between two signals was computed to obtain the correlation coefficient. Possible correlations range from +1 to –1. A zero correlation indicates that there is no relationship between the variables. A correlation of –1 indicates a perfect negative correlation, meaning that as one variable goes up, the other goes down. A correlation of +1 indicates a perfect positive correlation, meaning that both variables move in the same direction together.

5.3 Determination of underground water velocity

The one-dimension of velocity was calculated by using GMR signal. Because, the two GMRs have a fixed distance between them as described above, we can determine the one dimension of velocity. The one dimension velocity (m/s) equal distance difference (m) divided by time

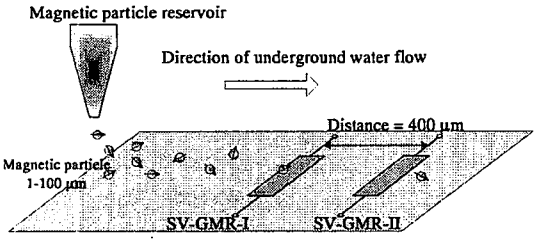

Figure 24 Model of underground water velocity measurement by GMR sensor.

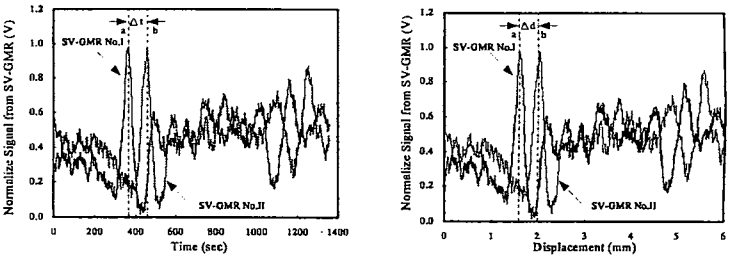

(a) Distance difference (b) Time difference

Figure 25 Detection of underground water velocity by GMR.

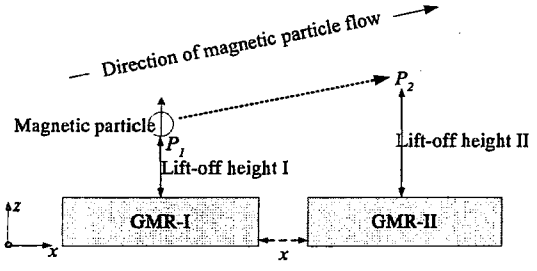

Figure 26 Lift-off height effects.

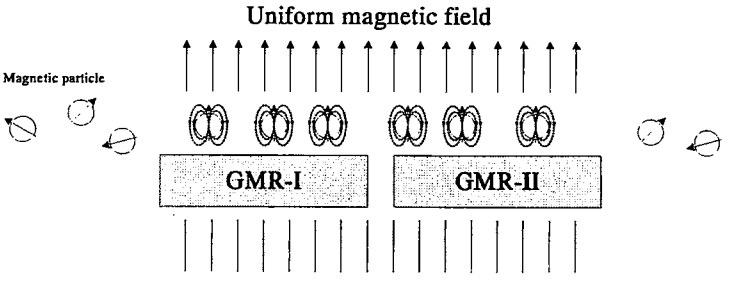

Figure 27 .Application of uniform magnetic fields to control dipole moment of magnetic particle.

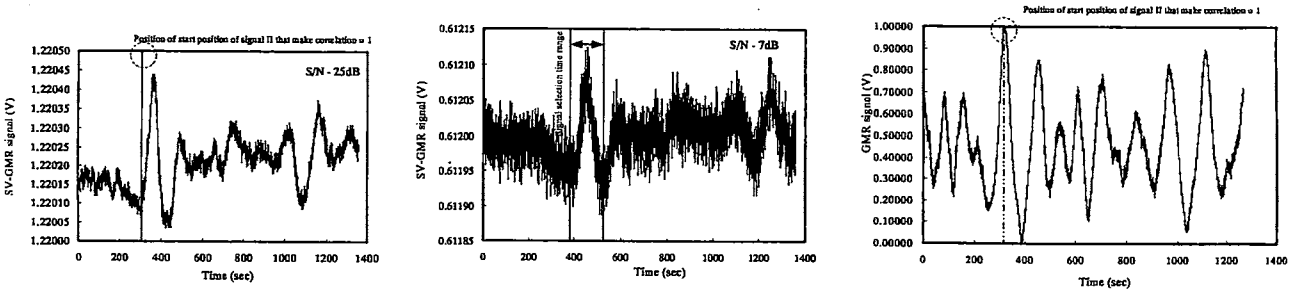

(a) GMR-I (b) GMR-II (c) Correlation

Figure 28 Simulation result in case of lift-off height effects.

difference (s). Figure 25 shows determination of underground water velocity by GMR signal. The result of one dimension velocity of this experiment is 14.4 x 10^{-6} m/s.

5.4 Simulation signal in case of lift-off height

It is difficult to predict the behavior of underground water as described above. In this technique one- dimension velocity detection is considered. There are some cases that we can simulate the signal such as for the lift-off height effect as shown in Figure 26. The lift-off height effect is height of magnetic particle change.

The raw signal of magnetic particle detection that is obtained from GMR I and II consists of the particle signal plus noise signal that is generated by GMR itself. Both of signals were added with noise signal which simulates environment effect such as contamination water, heat, flow pattern and etc. In this case, the Gaussian noise was applied to raw signal. The signal of GMR II was decreased because it has an effect from lift-off height of 50%. The normalization signal was applied to find out the correlation coefficient signal.

The method of correlation was computed in case of lift-of height simulation. The result shows in Figure 28. The matching position of start point of signal II is clearly positioned so that it makes the correlation coefficient equal 1.In addition, the uniform magnetic field is helping the dipole moment arrange in the same direction, which means the GMR can clearly verify the magnetic particle signal as shown in Figure 27.

7. Conclusion

The proposed ECT probe that was fabricated consists of the SV-GMR as a sensor and exciter. The flux concentrator, double spiral, Hemholtz coil and ferrite core were compared to detect the conductive microbead. The proposed ECT probe (flux concentrator) can improve the signal obtained from the SV-GMR sensor. Not only single conductive microbead but also ball grid array (BGA) is clearly detected with the proposed ECT probes. The result of FEM was calculated which agreed with the experimental result. One GMR clearly detects the magnetic particle model I to III. Two GMRs were applied for one dimension underground water velocity detection. The simulation technique was proved that in case of lift-off height the GMR can detect the signal of good level. The results of simulations and experimentations have shown a great potential for this technique in the future design and implementation.

8. References

[1] T. Somsak, K. Chomsuwan, S. Yamada, and M. Iwahara, "Conductive Microbead Array Detection Based on Eddy-Current Testing Using SV-GMR Sensor and Helmholtz Coil Exciter," *IEEE Transactions on Magnetics*, vol 42, no. 10, pp. 3572-3574, 2006.

[2] T. Somsak, K. Chomsuwan, S. Yamada, and M. Iwahara, "Spin-valve GMR Senser with Improved Ferrite core Exciter for Conductive Microbead Detection by Eddy-current Testing Technique," *Journal of the Magnetics Society of Japan*, vol.31, no.5, pp. 398-401, 2007.

[3] T. Somsak, K. Chomsuwan, S. Yamada, and M. Iwahara, "Utilization of SV-GMR for Detection Conductive Microbead with Helmhlotz Coil Exciter Based on Eddy Current Testing," *Journal of*

the Japan Society of Applied Electromagnetics and Machanics, vol. 15, no. 3, pp. 62-65, 2007.

[4] T. Somsak, K. Chomsuwan, S. Yamada, and M. Iwahara, "Conductive Microbead Detection by Helmholtz Coil Technique with SV-GMR," *DELTA 2006 Third IEEE International Workshop on Electronic Design, Test&Applications*, pp. 157-162, 2006.

[5] T. Somsak, K. Chomsuwan, S. Yamada, and M. Iwahara, "Detection of Conductive Microbead by ECT Probe with Flux Concentrator Exciter," *The 19th Symposium on Electromagnetics and Dynamics*, no. 07-253, pp. 251-254, 2007.

[6] T. Somsak, K. Chomsuwan, S. Yamada, and M. Iwahara, "Recognitions of Micro Non-Magnetic and Magnetic Material with GMR Sensor," *The 18th Symposium on Electromagnetics and Dynamics*, pp. 211-214, 2006.

[7] K. Chomsuwan, S. Yamada, T. Hagino, T. Somsak, and M. Iwahara, "Recognitions of Micro Non-Magnetic and Ferromagnetic Material with SV-GMR Sensor," *Proceeding of the 1st International Conference on Sensing Technology*, pp. 557-560, 2005.

[8] T. Somsak, K. Chomsuwan, S. Yamada, and M. Iwahara, "Underground Water Velocity Measurement by Magnetoresistance Sensor," *Digests of the 31st annual conference on magnetics*, pp.176 , 2007.

学位論文審査結果の要旨

当該学位論文に対して，平成20年1月30日に第1回論文審査委員会を開催し，同年1月31日に行われた口頭発表後に第2回論文審査委員会を開催し討議した結果，以下の通り判定した。

本研究は，プレーナ形コイルと巨大磁気抵抗効果素子(GMR)で構成したうず電流探傷(ECT)プローブによる導電性金属微粒子の検出特性とその応用に関するものである。磁気センサで構成したECT技術は，MHz以上の励磁周波数により nT の磁界感度と数10 μm程度の空間分解能を有することを明らかにし，その応用として電子回路の実装装置，低速の深地下水の速度計測について検討を行った。

主な成果は以下の通りである。

(1) 導電性金属微粒子の検出の理論的検討と高分解能ECTプローブの開発

解析的な検討により球状の導電性微粒子を含む微粒子のうず電流と周りの電磁界を求めることにより，対象とするハンダボール材料において100 μm以上の球に対して検出可能であることを明確にするとともに，磁気センサとプレーナコイルからなるマイクロECTプローブの具体的構成を検討した。

(2) 電子回路の表面実装用の微小ハンダボールの性状の検出

表面実装用のアレー状ハンダボールを対象にECTプローブによる非接触のボールの欠損，配置の実験的検討を行った。具体的には，励磁周波数5 MHzにより，125 μm以上において，位置精度の十分な情報を得られることを実証した。

(3) 深地下水速度の計測技術

深地下水に注入した微小金属浮揚体を2か所のECTプローブにより非接触で検出することにより，地下水速度を推定するシステムを提案し，流速 10^{-5} m/s オーダの計測下限値を得た。

以上の研究は，うず電流探傷技術による金属微粒子の検出の可能限界を明らかにし，その特色を生かした応用分野について検討したものであり，博士（工学）論文に値するものと判定した。